Resource

Cell Reports

APEX Fingerprinting Reveals the Subcellular Localization of Proteins of Interest

Graphical Abstract

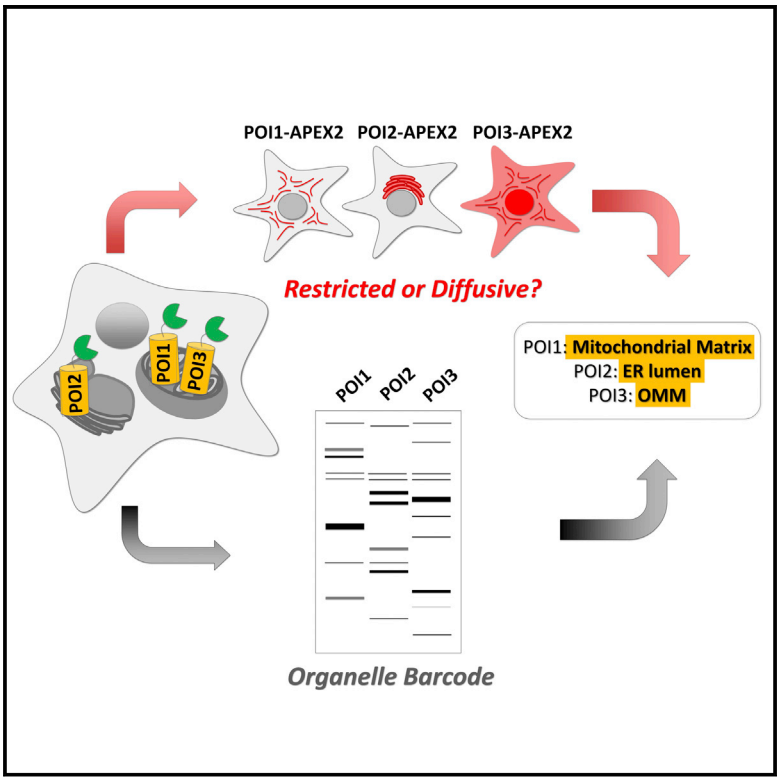

Authors

Song-Yi Lee, Myeong-Gyun Kang, Jong-Seok Park, Geunsik Lee, Alice Y. Ting, Hyun-Woo Rhee

Correspondence

ating@mit.edu (A.Y.T.), rhee@unist.ac.kr (H.-W.R.)

In Brief

Lee et al. examine subcellular localization at sub-compartmental resolution using APEX labeling of specific proteins. The method is used to reveal the sub-mitochondrial localization of recently identified mitochondrial proteins, as well as the membrane topology of the ER protein HMOX1.

Highlights

- Biotinylating proteins using APEX generates unique molecular patterns
- Molecular patterns provide sub-compartmental information about the APEX-tagged protein
- APEX labeling reveals HMOX1 membrane topology in the ER

Lee et al., 2016, Cell Reports *15*, 1–11
May 24, 2016
http://dx.doi.org/10.1016/j.celrep.2016.04.064

CellPress

Please cite this article in press as: Lee et al., APEX Fingerprinting Reveals the Subcellular Localization of Proteins of Interest, Cell Reports (2016), http://dx.doi.org/10.1016/j.celrep.2016.04.064

Cell Reports
Resource

APEX Fingerprinting Reveals the Subcellular Localization of Proteins of Interest

Song-Yi Lee,[1] Myeong-Gyun Kang,[1] Jong-Seok Park,[1] Geunsik Lee,[1] Alice Y. Ting,[2,*] and Hyun-Woo Rhee[1,*]
[1]Department of Chemistry, Ulsan National Institute of Science and Technology (UNIST), Ulsan 44919, Korea
[2]Department of Chemistry, Massachusetts Institute of Technology, Cambridge, MA 02139, USA
*Correspondence: ating@mit.edu (A.Y.T.), rhee@unist.ac.kr (H.-W.R.)
http://dx.doi.org/10.1016/j.celrep.2016.04.064

SUMMARY

Deciphering the sub-compartmental location of a given protein of interest may help explain its physiological function, but it can be challenging to do using optical or biochemical methods. Imaging with electron microscopy (EM) can provide highly resolved mapping of proteins; however, EM requires complex sample preparation and a specialized facility. Here, we use engineered ascorbate peroxidase (APEX)-generated molecular labeling patterns to provide information regarding intracellular microenvironments in living cells. Using APEX labeling of specific proteins, we uncovered subcellular localization at sub-compartmental resolution and successfully elucidated the membrane protein topology of HMOX1 and sub-mitochondrial localization of recently identified mitochondrial proteins. This method can be expanded to confirm sub-mitochondrial localization and membrane topologies of previously identified mitochondrial proteins.

INTRODUCTION

High-resolution protein mapping technologies have been used to provide detailed insight into the microenvironments of diverse cellular compartments (Martell et al., 2012; Rhee et al., 2013; Shim et al., 2012; Uhlen et al., 2010; Williams et al., 2014). Each cellular compartment contains varying protein compositions that underlie the diversity of biochemical reactions in a single cell. These compartments, or organelles, are further divided into sub-compartments. For example, mitochondria consist of three sub-compartments: the matrix, intermembrane space (IMS), and outer mitochondrial membrane (OMM) space. Even single endoplasmic reticulum (ER) membranes can have drastically different biochemical compositions on their cytosolic and luminal faces (Friedman et al., 2010; Shibata et al., 2006). Each of these sub-compartments plays a different role and hence contains a unique set of biomolecules. Therefore, it is important to determine the exact sub-compartment location of a particular protein to better understand its physiological function (Davis, 2004; Rees et al., 2015).

Identifying the subcellular localization of a protein of interest (POI) at the sub-compartment level is challenging using traditional optical or biochemical methods. Because of the low resolution of conventional optical imaging (~220 nm), the sub-organelle membrane localization of a POI cannot be distinguished (e.g., the distance between the inner-mitochondrial membrane [IMM] and the OMM is 15 nm). Even super-resolution imaging methods are unable to clearly distinguish protein topology on single organelle membranes (Shim et al., 2012). Additionally, biochemical methods that involve membrane perturbation with detergents or protease treatment of purified organelles may generate inaccurate findings because of inadequate purification and digestion techniques performed under non-physiological conditions, and thus the results can be inconsistent (Forner et al., 2006; Lorenz et al., 2006; Rees et al., 2015). Such a mistake in localization can lead to an inaccurate understanding of the physiological functions of a POI if placed in the context of inappropriate surrounding components (Koch et al., 2004; Medlock et al., 2015; Rhee et al., 2013).

Recently, a method for generating radicals in situ by engineered ascorbate peroxidase (APEX) was developed for target proteome profiling of sub-mitochondrial spaces (Chen et al., 2015; Hung et al., 2014; Rhee et al., 2013), the ER-PM junction (Jing et al., 2015), and primary cilia (Mick et al., 2015). APEX generates biotin-phenoxyl radicals in situ in the presence of hydrogen peroxide, and these short-lived radicals biotinylate neighboring proximal proteins in tight spaces because they have a small labeling radius (less than 20 nm) (Bendayan, 2001). Prior mass spectrometry analysis of the surrounding proteome of APEX-generated biotinylated proteins revealed various unknown proteins in the sub-mitochondrial proteome, further demonstrating that in-situ-generated radicals have a very short labeling radius. In this previous work, we recognized a "pattern" of short-lived biotin-phenoxyl radicals containing valuable information, not only for mass spectrometry analysis of the unknown surrounding proteome but also for identifying the exact location of a conjugated POI. For example, we found that the mitomatrix-APEX had a restricted biotin-labeling pattern because the mitochondrial matrix is surrounded by the impermeable IMM (Rhee et al., 2013), while a diffuse biotin-labeling pattern was observed by IMS-APEX (Hung et al., 2014) because OMM is porous to small molecules, such as biotin-phenoxyl radicals biotin-tagged proteins, and other molecules (Colombini, 1979). The results of IMS-APEX imaging may be due to their relocalization, rather than a long labeling radius of the biotin-phenoxyl radical (Hung et al., 2014). Furthermore, we found that mitomatrix- and IMS-APEX had distinct biotinylation patterns according to western

Please cite this article in press as: Lee et al., APEX Fingerprinting Reveals the Subcellular Localization of Proteins of Interest, Cell Reports (2016), http://dx.doi.org/10.1016/j.celrep.2016.04.064

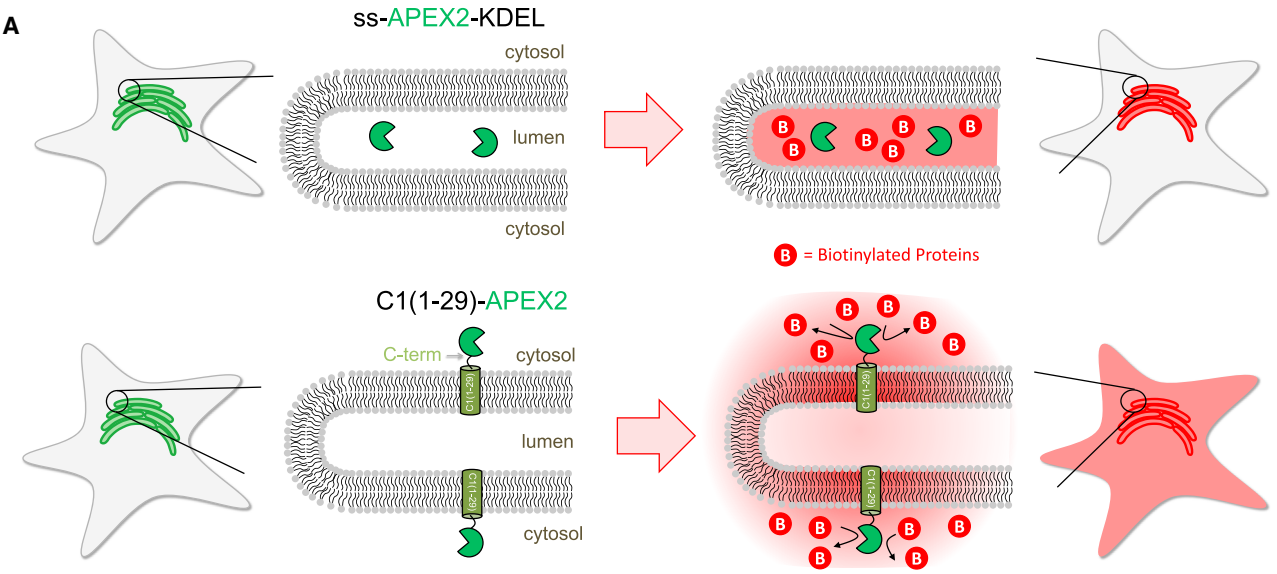

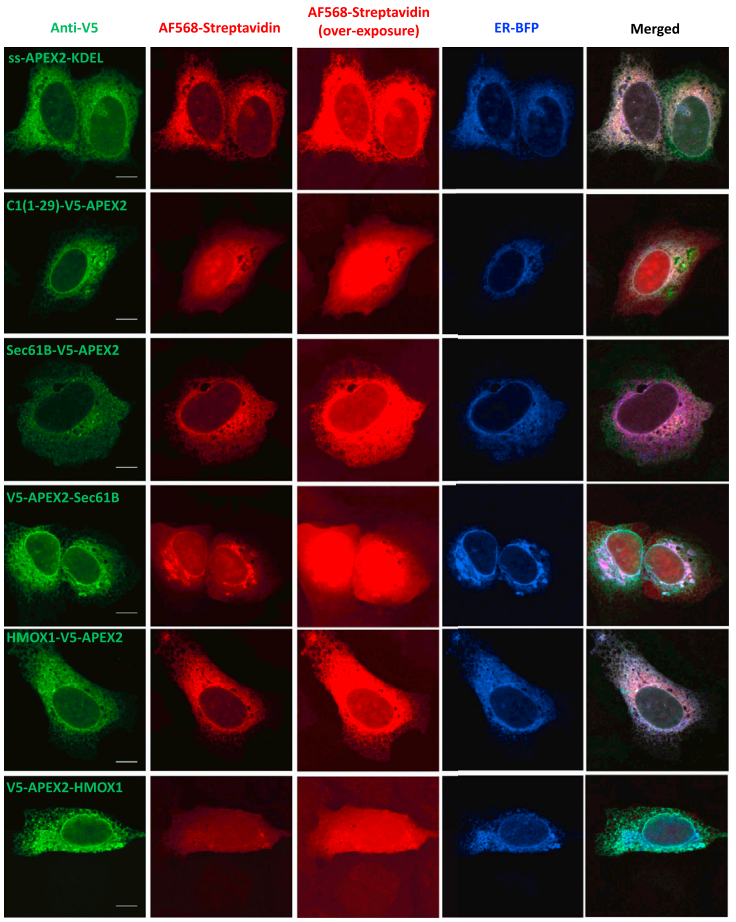

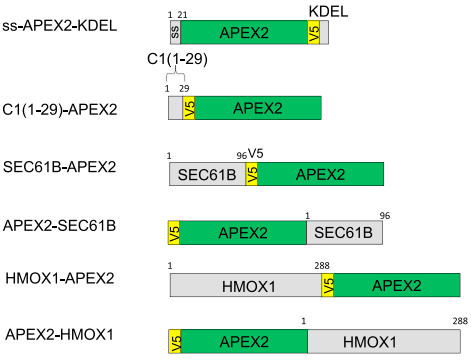

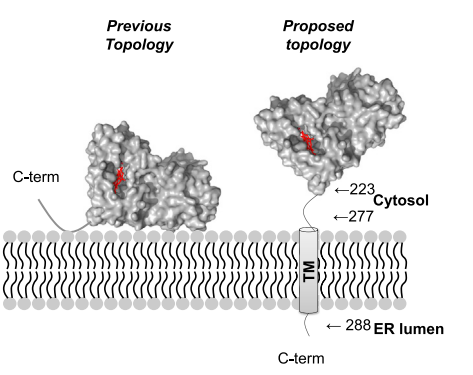

(legend on next page)

blot analysis. However, POI-APEX biotinylation patterns cannot be used as general indicators for the identification of POI location before systematic comparison of biotinylation patterns from other POI-APEXs in other organelles, such as the ER.

The ER is a single-layered membrane organelle involved in the generation of many secretory proteins and proteins along the secretory pathway. ER membranes separate the oxidative luminal space from the reductive cytosolic space. Transmembrane (TM) proteins in the ER membrane have at least two domains: the cytosolic and luminal domains, which interact with completely different subsets of peripheral membrane proteins. Therefore, it is crucial to determine the subcellular localization of each domain in order to correctly understand their functions. However, conventional biochemical methods and even recently developed super-resolution imaging methods are unable to provide sufficient resolution to discriminate whether target proteins or target sites are located on the cytosolic or luminal side (Shemesh et al., 2014). Therefore, we investigated whether this could be resolved based on the APEX-generated molecular labeling pattern in mammalian cell lines (e.g., HEK293T, HeLa, and U2OS cell).

RESULTS AND DISCUSSION

Characterization of Biotin-Phenol Labeling Pattern across the ER Membrane

First, we evaluated whether APEX-generated patterns were different in the luminal space compared to the cytosolic space of the ER. To accomplish this, we examined the biotinylation patterns of the ER luminal space-targeted APEX (ss-APEX2-KDEL) and the ER cytosolic face-targeted APEX (C1(1-29)-APEX2) (Kalderon et al., 1984). We used APEX2 for all experiments in this report, because APEX2 is a further engineered version of APEX with higher catalytic efficiency (Lam et al., 2015). As shown in Figure 1, different patterns of biotin labeling were clearly observed. APEX2-KDEL displayed a very ER-restricted biotin-labeling pattern. In contrast, C1(1-29)-APEX2 showed a very diffusive whole-cell biotin-labeling pattern in which the nuclear region was also heavily labeled with streptavidin-AF568. This same nuclear region was not labeled by the ER luminal-targeted APEX2 as observed even in the over-exposed imaged. Thus, we confirmed that "restricted or diffuse" biotin-labeling patterns (RD pattern) clearly indicate whether the APEX-tagged POI was on the inner membrane or outer membrane on the targeted organelle in a living cell.

ER Transmembrane Protein Topology Identification by APEX-Generated Pattern

APEX was further investigated for its ability to generate different biotin-labeling patterns when conjugated to different termini of single-pass ER membrane proteins. SEC61B, which is a single-pass ER TM protein that has a well-known topology with its N and C termini localized to the cytosolic side and luminal side, respectively, was used as a model (Friedman et al., 2010). As expected, APEX2-SEC61B (N-terminal tagging) and SEC61B-APEX2 (C-terminal tagging) generated notably different RD patterns, as shown in Figure 1. This RD pattern corresponded well to the previously known SEC61B topology on the ER membrane.

APEX was then used to determine the controversial membrane topology of the heme oxygenase 1 (HMOX1) protein (Gottlieb et al., 2012). The HMOX1 protein plays a crucial role in heme metabolism as it degrades heme to biliverdin and interacts with the amyloid beta precursor protein, which is related to Alzheimer's disease (Takahashi et al., 2000). HMOX1 is known to be an ER membrane protein; however, its membrane topology is unclear (Gottlieb et al., 2012). In Uniprot, HMOX1 is annotated as a peripheral ER membrane binding protein with no transmembrane domain, while earlier studies showed that HMOX1 has a C-terminal transmembrane domain. Thus, we generated APEX2-HMOX1 (N-terminal tagging) and HMOX1-APEX2 (C-terminal tagging) and imaged the RD pattern in U2OS cells. As shown in Figure 1B, APEX2-HMOX1 showed a diffuse biotin-labeling pattern, whereas HMOX1-APEX2 showed a restricted biotin-labeling pattern. These results imply that the N terminus of HMOX1 is exposed to the cytosol and the C terminus is located in the ER lumen. Moreover, electron microscopy (EM) imaging results (Figure S2) suggest that the C terminus of HMOX1 is in the ER lumen, similar to that of SEC61B. Our proposed topology of HMOX1 is shown in Figure 1D. Our proposed model of HMOX1 is consistent with the previously proposed tail-anchored model from other studies (Gottlieb et al., 2012; Yoshida and Sato, 1989).

Western Blot Analysis of Biotin-Labeled Pattern from Various POI-APEXs

In the above imaging experiments, biotin-labeling patterns were determined to be either diffuse or membrane restricted. Additionally, we found that streptavidin-horseradish peroxidase (SA-HRP)-stained western blots show diverse and unique patterns (Figure 2A). As shown in Figure 2B, the western blot patterns for APEX2 conjugated to nuclear, cytosolic, mitochondrial matrix, and IMS proteins were distinct. This unique biotin-labeling pattern may reflect a different inventory of proteins located in each of the subcellular compartments.

Interestingly, biotin-labeling patterns generated using two different APEX targeting sequences targeted to the same compartment showed remarkable similarities. For instance, the biotin-labeling patterns of TOM20-APEX2 (OMM) and APEX2-NES (cytosol) were very similar because both the C terminus of TOM20 and NES were localized in the cytoplasm and hence

Figure 1. Confocal Microscopy Imaging of Biotin-Labeling Patterns by Various ER-Localized POI-APEXs

(A) Scheme of restricted and diffusive biotin-labeling patterns.

(B) Confocal microscope imaging of biotin-phenol labeling patterns by various ER-localized POI-APEX2s in U2OS cells. Labeling was conducted in living cells, and imaging was conducted after fixation/permeabilization. Scale bar represnts 10 μm.

(C) Construct map of various ER-localized POI-APEX2s.

(D) Previous and proposed topology of HMOX1 based on our results. Previous topology information is from Uniprot (P09601). Crystal structure of soluble catalytic domain (10–233 amino acids) of HMOX1 is from protein database bank (PDB: 1N45). Heme is colored red in the structure.

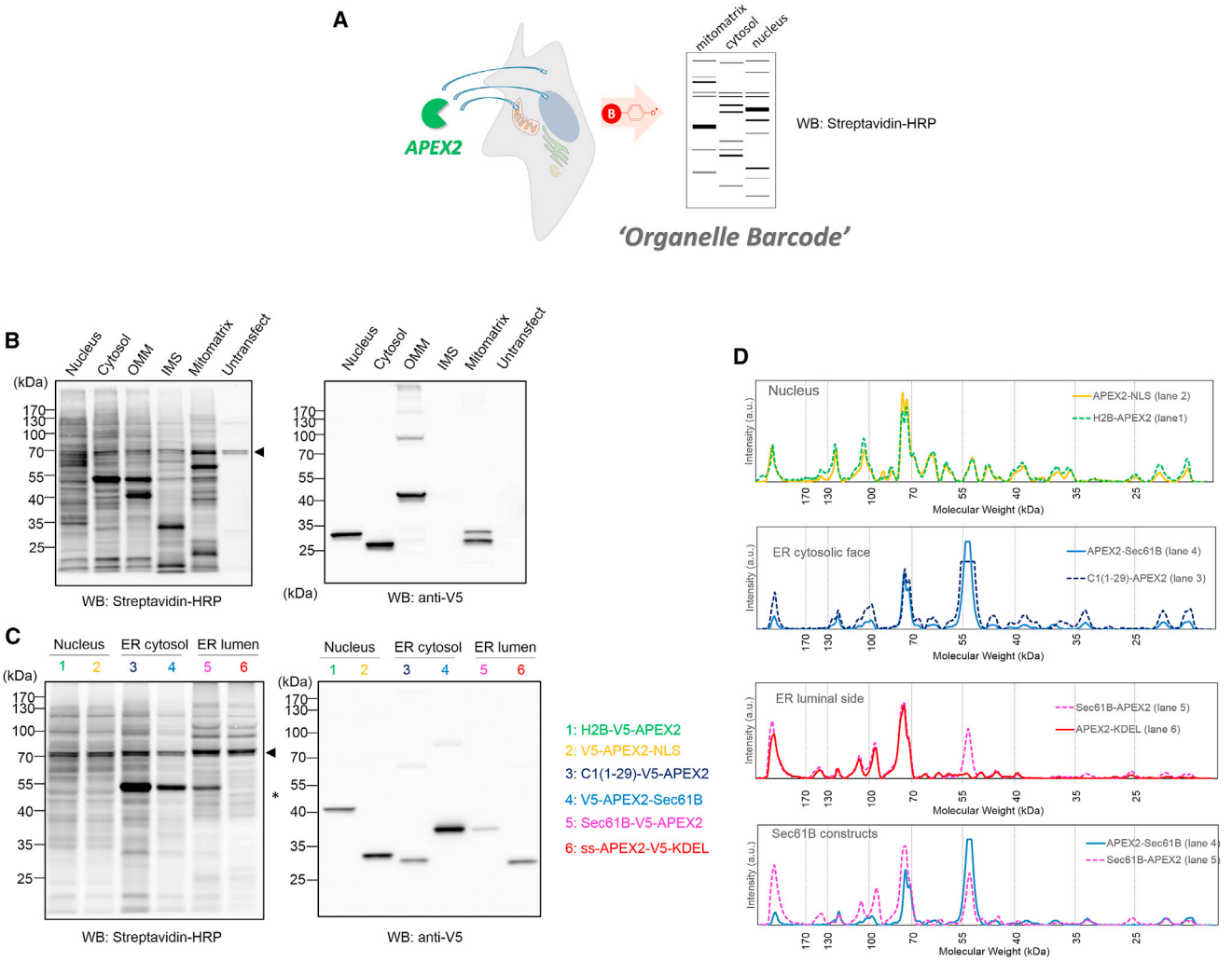

Figure 2. Organelle Barcode Generation of Various POI-APEXs

(A) Scheme of organelle barcode generation of different cellular organelle-targeted APEX2-tagged proteins. Different sizes and band intensities of biotin-phenol labeled proteins by various POI-APEX2-generated barcode-like patterns in streptavidin-HRP western blots.

(B) SA-HRP detection of biotinylated proteins of APEX2s from various subcellular compartments, including cytosol by V5-APEX2-NES, nucleus by V5-APEX2-NLS, OMM by TOM20-V5 APEX2, IMS by LACTB-Flag-APEX2, and Mitomatrix by Mito-V5-APEX2. V5 epitope tag detection of the expressed enzyme is shown to the right; LACTB-Flag-APEX2 was not detected because it had a Flag tag.

(C) SA-HRP detection of biotinylated proteins from various nuclei and ER-APEX2 constructs (left) and anti-V5 western blot (right). The arrow indicates endogenous biotinylated proteins and the asterisk indicates biotinylated tubulin proteins.

(D) Line-scan analysis graph of SA-HRP western blot of (C).

labeled as the same milieu cytosolic proteins (Figure 2B). Furthermore, H2B-APEX2 and APEX2-NLS were targeted to the nucleus using different targeting sequences, and their molecular patterns were very similar (Figure 2C). This similarity was also recognized when blot images were converted to a line-scan analysis graph (x axis: molecular weight, y axis: band intensity) as shown in Figure 2D. Therefore, the unique biotin-labeling pattern of each subcellular compartment, referred to as the "organelle barcode" (Figure 2A), is a strong predictor of the origin of a protein.

To determine whether the organelle barcodes can be used as indicators for membrane topology, the biotin-labeling pattern of four ER-targeted POI-APEXs (APEX2-KDEL, C1(1-29)-APEX2, SEC61B-APEX2, APEX2-SEC61B) were evaluated. The barcodes were very homologous among the groups of proteins from the same sub-compartments (i.e., lumen or cytosol), which were previously determined based on RD patterns (Figures 2C and 2D). We think that the strongly labeled protein in lanes 3, 4, and 5 (Figure 2C) might be a tubulin protein because it is known that ER is mainly supported by physical interaction with the microtubular network (Friedman et al., 2010). Furthermore, the fact that the observed molecular weight of tubulin is 55 kDa also supports this hypothesis. The reason why Sec61B-APEX2 (lane 5, Figure 2C) can label tubulin protein

might be that Sec61B is a subunit of a translocon channel that is porous for small molecules (Heritage and Wonderlin, 2001). Thus, we postulate that biotin-phenoxyl radicals that slightly leaked from SEC61B-APEX2 can react with tubulin at the ER cytosolic face (Friedman et al., 2010).

Furthermore, the organelle barcode of HMOX1-APEX2 was similar to that of SEC61B-APEX2, and the barcode of APEX2-HMOX1 was similar to that of APEX2-SEC61B, indicating that HMOX1 has the same orientation as SEC61B (Figure S1). We also used APEX-EM imaging methods with these constructs. Both the SEC61B-APEX2- and HMOX1-APEX2-diaminobenzidine (DAB)-labeled regions were on the ER lumen (Figure S2), which also supports our proposed membrane topology of HMOX1 on the ER membrane (Figure 1D). There are several suggested mechanisms for ER transport of tail anchored (TA) membrane proteins (Hegde and Keenan, 2011). However, how TA substrates are inserted into the ER membrane is still elusive. We think that our C term-tagged APEX2 results may suggest that membrane insertion mechanism of SEC61B and HMOX1 should not be followed by spontaneous pathway (Brambillasca et al., 2005). Thus, in the future, it might be intriguing to investigate the translocation pathway that HMOX1 and Sec61B are following during ER transport.

Overall, the microscopy and western blot results of APEX-generated molecular patterns showed good agreement, and both methods are useful for identifying the sub-compartmental localization of POI.

Quantitative Barcode Analysis for Identifying Sub-organelle Spaces of Mitochondrion

Because APEX-generated biotinylation patterns show highly distinguishable resolution across single organelle membranes, this method was expanded to identify the sub-compartmental identification of mitochondrial POIs in mitochondrion in which sub-compartmental information is particularly important to understand their physiological roles. To examine this point, the C termini of several mitochondrial proteins were APEX2-tagged (PDK1 [matrix], SCO1 [IMS], and TOM20 [OMM]); their sub-compartmental locations within the mitochondria are well-documented. Microscopy imaging experiments demonstrated that PDK1-APEX2 had a restricted biotin-labeling pattern that was the same as Mito-APEX2 (mitochondrial matrix), and SCO1-APEX2 and TOM20-APEX2 had diffuse patterns similar to LACTB-APEX2 (IMS) (Figure S3). Additionally, organelle barcodes obtained by western blotting showed high similarity to barcodes from standard APEX2-tagged proteins with known compartmental localization (Mitomatrix, LACTB [IMS], and NES) (Figure 3A). To quantify these results, a western blot image was converted to a line-scan analysis graph (Figure 3B), and correlation values of each graph with others were scored as barcode correlation values (highest, 1; lowest, 0) using the correlative function (see the Experimental Procedures). For example, the PDK1 to mitomatrix correlation value was 0.90, and the PDK1 to LACTB correlation value was 0.34. Additionally, the SCO1 to LACTB correlation value was 0.83, and the SCO1 to matrix correlation value was 0.38 (Figure 3C). We found that the correlation values for these model proteins were strong predictors of their locations and therefore applied them to predict the sub-compartmental localization of the newly identified mitochondrial proteins TRMT61B and MGST3.

TRMT61B and MGST3 are newly identified mitochondrial proteins and their sub-compartmental localization has not been confirmed (Hung et al., 2014; Rhee et al., 2013). Thus, we conjugated APEX2 to the C terminus of these proteins and examined the RD patterns and organelle barcodes. As shown in Figure 3D, the biotin-labeling pattern of TRMT61B-APEX2 was membrane restricted, whereas the biotin-labeling pattern of MGST3-APEX2 was diffuse. This strongly suggests that TRMT61B is localized in the mitochondrial matrix, and MGST3 was either in the IMS or OMM. The exact sub-compartmental localization of MGST3 (i.e., IMS or OMM) in the mitochondrion could not be solely determined through microscopy image analysis because the diffuse biotin-labeling patterns from both sub-compartments were very similar. Thus, we analyzed the organelle barcodes of MGST3-APEX2 to determine whether this protein localizes to the IMS or OMM. Barcodes of MGST3-APEX2 were compared to other APEX-generated barcodes of standard proteins, including mitomatrix, LACTB (IMS), TOM20 (OMM), NES (cytosol), and well-known sub-mitochondrial proteins (PDK1 and SCO1). Quantitative correlation analysis revealed that the barcode of MGST3 had high-correlation values with the barcodes of TOM20 (0.82) and NES (0.88) and low-correlation values with SCO1 (0.38) and LACTB (0.49), indicating that the C terminus of MGST3 was localized on the OMM. Furthermore, the barcode of TRMT61B showed high-correlation values with standard matrix (0.76) and PDK1 (0.81), confirming that TRMT61B was localized to the mitochondrial matrix. Based on the correlation value of barcodes and RD pattern analysis, the C terminus of TRMT61B is localized in the matrix, while the C terminus of MGST3 is localized at the OMM (Figure 4D).

To confirm the predicted sub-mitochondrial localization of TRMT61B and MGST3, we performed transmission electron microscopy (TEM) imaging of TRMT61B-APEX2, MGST3-APEX2, and SCO1-APEX2 as an IMS control using the APEX-EM method (Lam et al., 2015; Martell et al., 2012). As shown in Figure 3E, MGST3-APEX2 was clearly localized on the OMM, while TRMT61B-APEX2 was localized in the matrix. Overall, these results demonstrate that the APEX-generated molecular pattern predictions matched the TEM imaging results.

Notably, MGST3 was recently identified as a mitochondrial protein in a recently mapped IMM/IMS/OMM proteome list by IMS(LACTB)-APEX (Hung et al., 2014). MGST3 was shown to be an ER protein; however, our method clearly demonstrated that MGST3 is localized at the OMM. By using monoclonal antibody for MGST3, we also confirmed that endogenous MGST3 is localized at the mitochondria by confocal microscopic imaging (Figure S7) and is clearly localized at the OMM by EM imaging (Figure S8). Thus, our results suggest that the previous annotation of MGST3 as a microsomal protein in the secretory pathway should be revised to be a mitochondrial protein at the OMM.

TRMT61B was recently detected in the mitochondrial matrix proteome list by using mitomatrix-APEX, but no subsequent studies have confirmed whether it is localized in the mitochondrial matrix. In this study, all of our APEX-generated pattern/EM results and previously APEX-mediated proteome mapping results were in good agreement and demonstrated that

Please cite this article in press as: Lee et al., APEX Fingerprinting Reveals the Subcellular Localization of Proteins of Interest, Cell Reports (2016), http://dx.doi.org/10.1016/j.celrep.2016.04.064

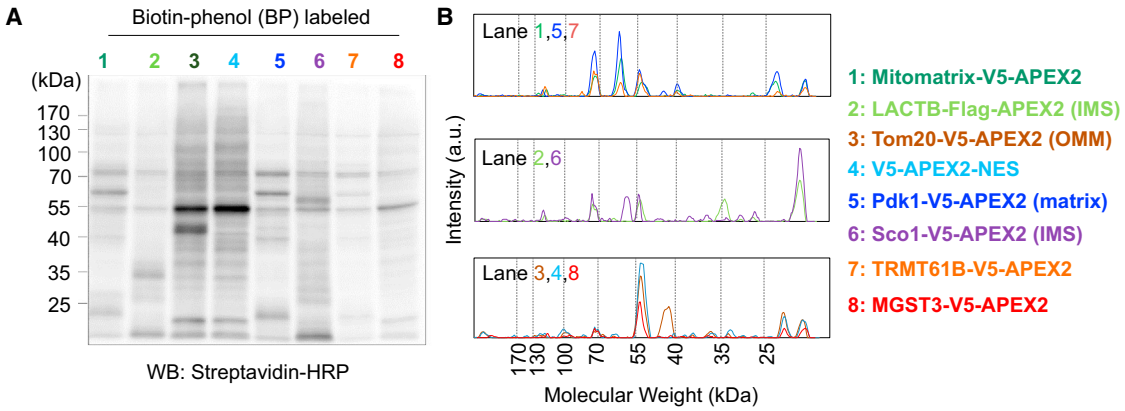

C

	matrix (1)	LACTB (2)	Tom20 (3)	NES (4)	Pdk1 (5)	Sco1 (6)	TRMT61B (7)	MGST3 (8)
matrix (1)	1	0.35	0.33	0.40	0.90	0.38	0.76	0.42
LACTB (2)		1	0.45	0.44	0.34	0.83	0.48	0.49
Tom20 (3)			1	0.85	0.34	0.35	0.54	0.82
NES (4)				1	0.37	0.31	0.59	0.88
Pdk1 (5)					1	0.32	0.8	0.42
Sco1 (6)						1	0.41	0.38
TRMT61B (7)							1	0.71
MGST3 (8)								1

0.3 1.0
Barcode correlation value

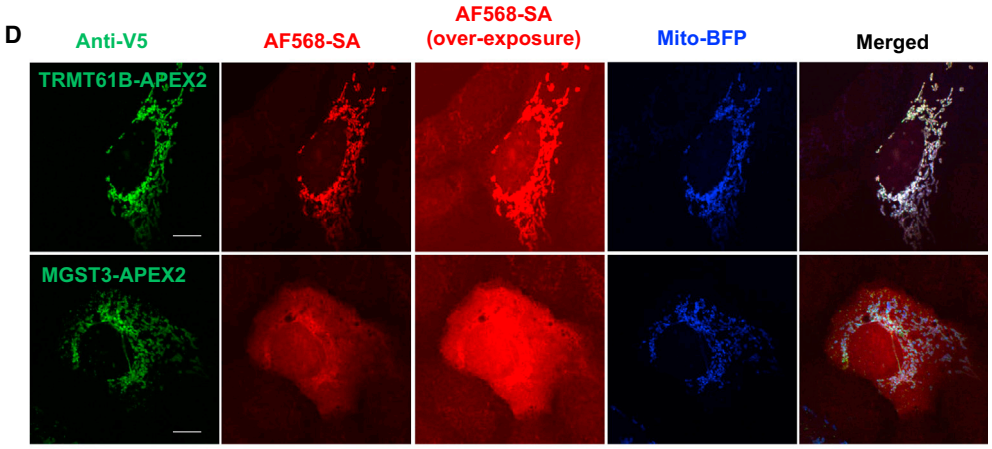

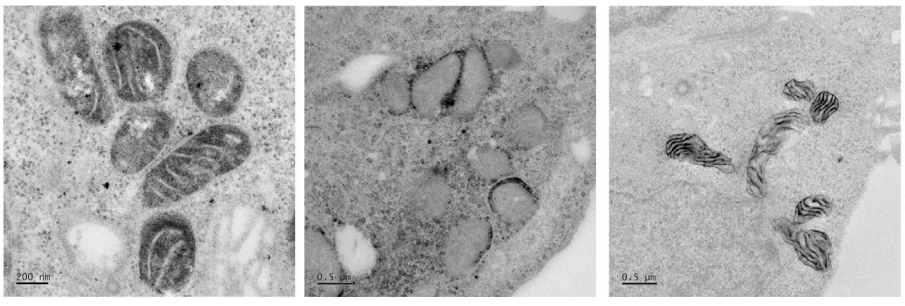

(legend on next page)

TRMT61B is a mitochondrial matrix protein. This result also suggests that the proteins with no sub-mitochondrial annotation in the recently sub-mitochondrion proteome list (265 proteins in mitomatrix-APEX's list [Rhee et al., 2013]; 55 proteins in IM-S-APEX's list [Hung et al., 2014]) belong in the same space to that in which the APEX is targeted.

APEX Pattern Method Identified Sub-mitochondrial Spaces of Several Mitochondrial Proteins

In Mitocarta, a gold list of whole-mitochondrial proteins in mammals (Pagliarini et al., 2008), several hundred mitochondrial proteins whose sub-mitochondrial localizations have not been completely annotated are listed. Thus, we further expanded our study to identify sub-mitochondrial locations of some of these unannotated sub-mitochondrial proteins. To identify sub-mitochondrial protein localization, we selected 12 mitochondrial proteins (AURKAIP1 [Koc et al., 2013], BIT1/PTRH2 [Jan et al., 2004], COX14 [Mick et al., 2010], MRPL12 [Surovtseva et al., 2011], MRM1 [Lee et al., 2013], MRPS15 [Cavdar Koc et al., 2001], PLGRKT [Andronicos et al., 2010], QIL1/MIC13 [Guarani et al., 2015], SFXN1 [Fleming et al., 2001], SVH/ARMC10 [Serrat et al., 2014], and TRMT2B) and conjugated APEX to the C terminus of each protein. Based on imaging experiments, we found that expression patterns of all APEX2 constructs overlapped well with the mitomarker, Mito-BFP, indicating that mitochondrial targeting of these proteins was not compromised by APEX tagging (Figure 4). Among these proteins, five proteins (MRPL12, MRPS15, TRMT2B, MRM1, and AURKAIP1) showed very restricted biotin patterns (Figure 4A), and thus we classified these proteins as mitochondrial matrix proteins based on imaging assays. For proteins showing diffusive biotin-labeled patterns, their organelle barcodes were analyzed by a correlation method with the standard organelle barcodes of SCO1 (IMS) and NES (cytosol) (Figure 4B). Based on the barcode correlation value shown in Figure 4C, we suggested that the C termini of SFXN1, QIL1/MIC13, and PLGRKT are localized in the IMS, and the C termini of SVH, COX14, and BIT1/PTRH2 are localized at the OMM. Our suggested localization of the C terminus of each protein is summarized in Figure 4D.

SFXN1 is a mitochondrial iron transporter protein directly linked to mitochondrial iron metabolism (Fleming et al., 2001) and whose sub-mitochondrial localization has not been characterized. In this study, we found that the C terminus of SFXN1 was localized at the IMS. QIL1/MIC13 is a recently identified interacting component with the MICOS complex (Guarani et al., 2015) and is known to be localized in the IMS; our results clearly showed that its C terminus localizes in the IMS. PLGRKT is known to be localized at the plasma membrane (Andronicos et al., 2010); however, our results suggest that this is a mitochondrial protein whose C terminus was localized in the IMS. Its IMS correlation is more clearly shown in the correlation values of a low-molecular-weight barcode less than 55 kDa, and all the predicted IMS-localized proteins also showed values more correlative with each other at this range. As shown in a line-scan analysis graph of these POIs, strong labeled protein signals below 25 kDa generate a high correlative score (Figure S4). We hypothesize that abundant small-size protein population in IMS (e.g., cytochrome *c*) might generate this unique signature of IMS barcode.

SVH/ARMC10 is known to interact with MIRO-1 and MIRO-2 at the OMM (Serrat et al., 2014), and we confirmed its OMM localization based on its high barcode correlation value with APEX2-NES. BIT1/PTRH2 is known to play an important role in controlling apoptosis on the OMM (Jan et al., 2004), and we confirmed its OMM localization based on its barcode. In the case of COX14, previous biochemical assays revealed that its C terminus is exposed in the IMS (Mick et al., 2010); however, our results showed that its C terminus is exposed in the cytosol. All these OMM-predicted POIs also showed higher correlation values with each other than with IMS-predicted POIs (Figure 4C).

TRMT2B is first observed to be localized in mitochondrial matrix in our study. MRPL12 (Surovtseva et al., 2011) and MRM1 (Lee et al., 2013) are associated with mitochondrial RNA polymerase and the mitochondrial nucleoid complex, respectively, and MRPS15 (Cavdar Koc et al., 2001) and AURKAIP1 (Koc et al., 2013) are known to be components of the mitochondrial ribosome complex. Because all of these protein complexes are localized in the mitochondrial matrix, they are likely targeted to the matrix. Our APEX pattern results confirmed that MRPL12, MRPS15, MRM1, and AURKAIP1 were localized in the mitochondrial matrix. Our C-terminal mapping results are summarized in Figure 4D. Additionally, taking the predicted transmembrane domains and our identified C-termini localization into consideration, we propose the membrane topology of several known transmembrane proteins (Figure S6).

In this study, we demonstrated that our proposed APEX-generated molecular pattern recognition method is a general method for the identification of POI localization and membrane topology. Notably, several reported membrane topology mapping methods have used enzymatic glycosylation in living cells (Kim et al., 2006; Lee et al., 2012). However, these methods may be limited to the membrane proteins within the secretory pathways in which glycosyl modification occurs. Compared to this method, our APEX pattern method can be applied to various organelles in mammalian cells.

Figure 3. Sub-mitochondrial Localization of TRMT61B and MGST3 via Tagged APEX-Generated Biotin-Labeling Pattern Recognition

(A and B) SA-HRP western blot image of the labeled proteins from whole-cell lysates of various mitochondrial POI-APEX2 with 500 μM biotin-phenol (A) and its line-scan analysis graph (B).

(C) Table of calculated barcode correlation values of organelle barcodes (A and B).

(D) Confocal microscope imaging of the biotin-labeling patterns of TRMT61B-V5-APEX and MGST3-V5-APEX. Green fluorescence represents immunofluorescence of enzyme expression (Alex Fluor 488 anti-mouse conjugate/anti-V5 detection), and red fluorescence detects biotin-labeled proteins (Alexa Fluor 568 streptavidin conjugate detection). Labeling was conducted in living cells, and imaging was conducted after fixation/permeabilization. Scale bar represents 10 μm.

(E) Electron microscopic imaging of TRMT61B-APEX2, MGST3-APEX2, and SCO1-APEX2. Scale bar represents 200 nm for TRMT61B-APEX2 image and 0.5 μm for MGST3-APEX2 and SCO1-APEX2 images.

Please cite this article in press as: Lee et al., APEX Fingerprinting Reveals the Subcellular Localization of Proteins of Interest, Cell Reports (2016), http://dx.doi.org/10.1016/j.celrep.2016.04.064

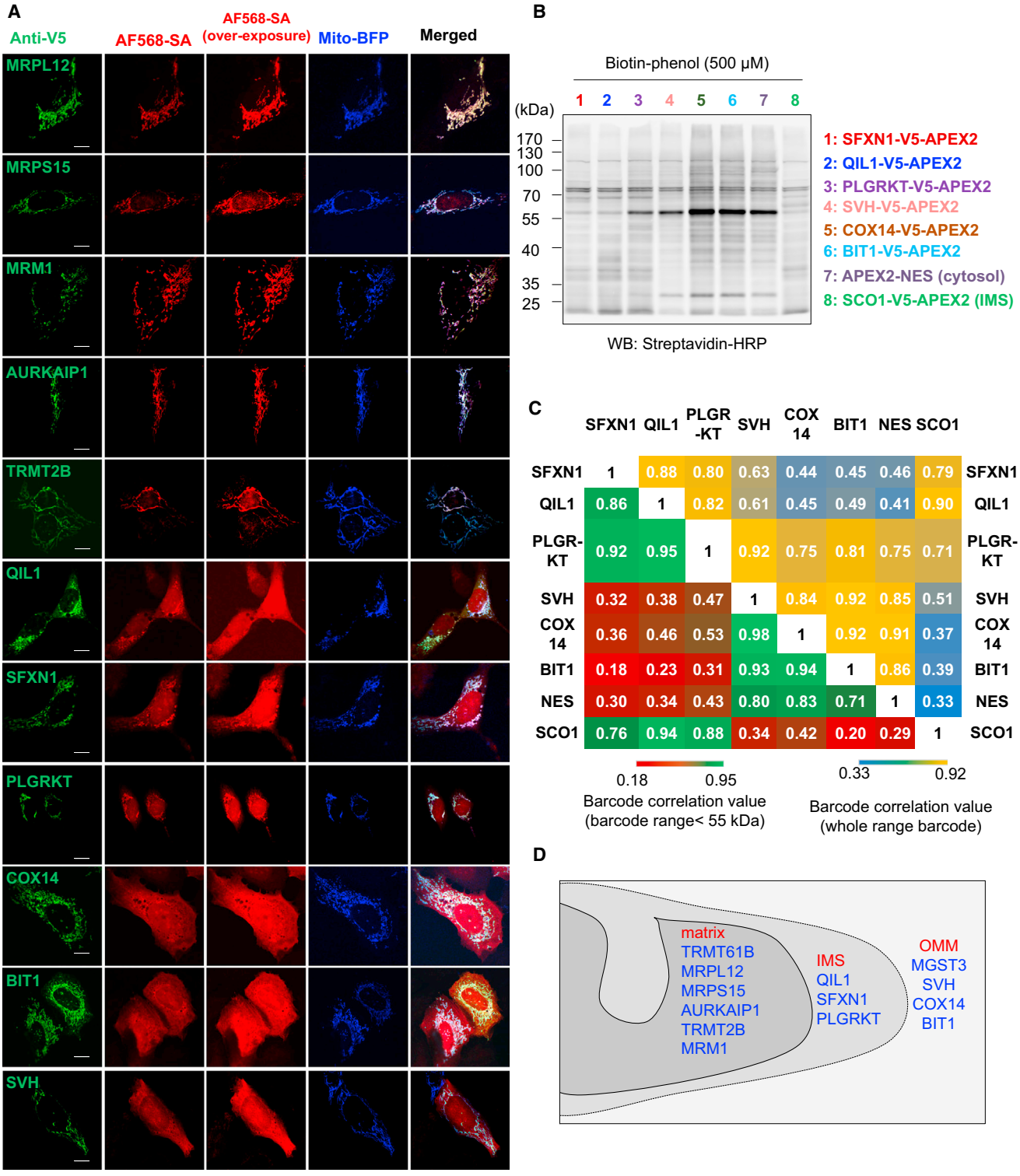

Figure 4. Sub-mitochondrial Space Mapping of Several Mitochondrial Proteins

(A) Confocal microscope imaging of the biotin-labeling patterns of various mitochondrial POI-V5-APEX2. Green fluorescence represents immunofluorescence of enzyme expression (Alexa Fluor 488 anti-mouse conjugate/anti-V5 detection), and red fluorescence detects biotin-labeled proteins (Alexa Fluor 568 streptavidin conjugate detection). Labeling was conducted in living cells, and imaging was conducted after fixation/permeabilization. Scale bar represents 10 μm.

(legend continued on next page)

Similar to the APEX-EM methods, our APEX pattern method can be used to provide very highly resolved mapping results. APEX-EM methods are useful for identifying sub-compartment localization of a POI in a fixed-cell state, and APEX fusion constructs were successfully employed to clearly identify the membrane topology of MCU (Martell et al., 2012) and MICU1(Lam et al., 2015). However, EM imaging requires complicated sample preparation, including embedding, sectioning, and imaging by well-trained scientists in a TEM facility. In this study, we found that the APEX pattern method in living cells also provided highly qualified mapping results with simple sample preparation steps. Furthermore, APEX pattern methods are easy to employ using a conventional fluorescence microscope and western blotting instruments in any molecular biology laboratory.

Conclusions

In the current study, we demonstrated that APEX-generated molecular pattern recognition is a robust method for providing high-resolution sub-organelle localization information of a POI. Using this method, we successfully identified the membrane topology of HMOX1 on the ER membrane and sub-mitochondrial localization of MGST and TRMT61B, as well as several other mitochondrial proteins. Our method could be useful to the biology research community because it is easy to implement and provides an efficient solution to determining membrane topology and sub-organelle protein localization.

EXPERIMENTAL PROCEDURES

Biotin-Phenol Labeling in Live Cells

Genes were introduced into HEK293T or U2OS cells through transient transfection with Lipofectamine 2000 (Life Technologies). After 18–24 hr (transfection), the medium was changed to 1 ml of fresh growth medium containing 500 μM biotin-phenol. This culture was incubated at 37°C under 5% CO_2 for 30 min in accordance with previously published protocols. Next, 110 μl of 10 mM H_2O_2 (diluted from 30% H_2O_2, H1009, Sigma Aldrich) was added to each well for a final concentration of 1 mM H_2O_2, and the plate was gently agitated for 1 min at room temperature. The reaction was then quenched by washing three times with Dulbecco's PBS (DPBS) containing 5 mM Trolox, 10 mM sodium azide, and 10 mM sodium ascorbate; then lysis was performed for western blot analysis, or fixation was performed for imaging analysis.

Western Blot Analysis of Biotin-Phenol Labeling

Cells were labeled under the same conditions described for the biotin-phenol labeling above. Then cells were lysed with RIPA lysis buffer containing 1× protease cocktail, 1 mM PMSF, 10 mM sodium azide, 10 mM sodium ascorbate, and 5 mM Trolox for 10 min at 4°C. Lysates were transferred to e-tube and clarified by centrifugation at 15,000 × *g* for 10 min at 4°C before separation on a 10% SDS-PAGE gel. For blotting analysis, gels were transferred to nitrocellulose membrane and blocked with 2% (w/v) dialyzed BSA (dBSA) in TBST (0.1% Tween-20 in Tris-buffered saline) at 4°C overnight or at room temperature for 1 hr. The blots were immersed in streptavidin-HRP in 2% dialyzed BSA in TBST (1:10,000 dilution, Thermo Scientific, cat. no. 21126) at room temperature for 30–60 min and then rinsed with TBST before development with Clarity reagent (Bio-Rad) and imaging on an ImageQuant LAS 4000 (GE healthcare).

Fluorescence Microscope Imaging

Biotin-labeled cells were fixed with 4% paraformaldehyde solution in DPBS at room temperature for 15 min. Cells were then washed with DPBS three times and permeabilized with cold methanol at –20°C for 5 min. Cells were washed again three times with DPBS and blocked for 1 hr with 2% dBSA in DPBS at room temperature.

To detect APEX2-fusion expression, the primary antibody, such as anti-V5 (Invitrogen, cat. no. R960-25, 1:5,000 dilution) or anti-Flag (Sigma Aldrich, cat. no. F1804, 1:3,000 dilution), was incubated for 1 hr at room temperature. After washing four times with TBST each 5 min, cells were simultaneously incubated with secondary Alexa Fluor 488 goat anti-mouse immunoglobulin G (IgG) (Invitrogen, cat. no. A-11001, 1:1000 dilution) and streptavidin-Alexa Fluor 568 IgG (Invitrogen, cat. no. S11226, 1:1000 dilution) for 30 min room temperature. Cells were then washed four times with TBST each 5 min and maintained in DPBS on ice for imaging by FV1000SPD (Olympus) of UOBC in UNIST, Korea.

Line-Scan Analysis and Correlation Value Calculation

Barcodes of streptavidin-HRP western blot images of Figures 3 and 4 were scanned and analyzed using ImageJ software (NIH) after background subtraction (ball-point size: 10 pt for Figure 3A and 30 pt for Figure 4B) was applied in the software. The resultant graph is shown in Figures 3B and S4. For quantification, we introduced the correlation index C_{ij} to quantify similarity between two barcodes *i* and *j*. For the given evenly spaced density values $\rho_0, \rho_1, \ldots, \rho_N$, $I_i(k)$ for a barcode *i* indicates the concentration with the mass density ranging ρ_{k-1} to ρ_k. Given a pair of the barcodes $I_i(k)$ and $I_j(k)$, the correlation C_{ij} is defined as shown in Equation 1.

$$C_{ij} = \frac{\frac{1}{N}\sum_{k=1}^{N} I_i(k) I_j(k)}{\sqrt{\frac{1}{N}\sum_{k=1}^{N} I_i(k)^2}\sqrt{\frac{1}{N}\sum_{k=1}^{N} I_j(k)^2}}. \quad (1)$$

This Equation 1 gives a greater or smaller value when two barcode shapes are more or less similar, respectively, and two identical barcodes result in a maximum value. The result is shown in Figures 3C and 4C.

TEM Imaging

HEK293T cells were grown on six-well cell culture plates. Cells were fixed on ice using cold 4% formaldehyde (Electron Microscopy Sciences) in PBS buffer for 15 min. All subsequent work was performed using pre-chilled buffers and reagents. Cells were again washed with PBS three times. DAB staining was initiated by adding freshly diluted 1 mg/ml (2.8 mM) DAB (Sigma; from a stock of the free base dissolved in 0.1 M HCl) and 10 mM H_2O_2 in PBS. After 20 min, the reaction was stopped by removing the DAB solution, and the cells were again washed with PBS 3 × 5 min each. Cells were then imaged by bright-field microscopy. Acquisition times ranged from 50 to 100 ms. For MGST3-APEX2 and ScoI-APEX2 EM, as shown in Figures 3E and S2, transiently transfected cells were grown in plastic six-well plates to 90% confluence, fixed using room temperature 2% glutaraldehyde (Electron Microscopy Sciences) in PBS and then quickly moved to ice. Cells were kept on ice for all subsequent steps until resin infiltration. After 30–60 min, the cells were rinsed 5 × 2 min each in chilled buffer and then treated for 5 min in buffer containing 20 mM glycine to quench the unreacted glutaraldehyde, followed by another 3 × 5 min rinses in chilled buffer. A freshly diluted solution of 1 mg/ml (2.8 mM) DAB free base was combined with 10 mM H_2O_2 in chilled buffer, and the solution was added to cells for 20 min. To halt the reaction, we removed the DAB solution and the cells were rinsed 3 × 5 min with chilled buffer. Post-fixation staining was performed using 2% (w/v) osmium tetroxide (Electron Microscopy Sciences) for 1 hr in chilled buffer. Cells were rinsed 5 × 2 min each in chilled distilled water. Cells were brought to room temperature, washed in distilled water, and then carefully scraped off the plastic,

(B) SA-HRP western blot image of the labeled proteins from whole-cell lysates of various mitochondrial POI-APEX2.
(C) Table of calculated barcode correlation value of organelle barcodes (B). Top-left part table is from whole-range barcode correlation (blue-yellow color-code), and down-left part table is from barcode correlation in the range of lower molecular weight proteins less than 55 kDa (red-green color-code).
(D) Sub-mitochondrion localization of C termini of mitochondrial POIs characterized in this study.

Please cite this article in press as: Lee et al., APEX Fingerprinting Reveals the Subcellular Localization of Proteins of Interest, Cell Reports (2016), http://dx.doi.org/10.1016/j.celrep.2016.04.064

resuspended, and centrifuged at 1,600 × *g* for 1 min to generate a cell pellet. The supernatant was removed, and the pellet was dehydrated in a graded ethanol series (50%, 60%, 70%, 80%, 90%, and 100%) for 15 min each time; then it was infiltrated into EMBED-812 (Electron Microscopy Sciences) using 1:1 (v/v) resin and anhydrous ethanol for 1 hr. The second change of 2:1 (v/v) resin and anhydrous ethanol was incubated overnight. After removing the resin, the sample was exchanged once more with 100% resin for 2 hr before transferring the sample to fresh resin, followed by polymerization at 60°C for 24 hr. Embedded cell pellets were cut with a diamond knife into 50-nm sections and imaged on a FEI-Tecnai G2 Spirit bio transmission electron microscope (operated at 120 kV) at the Korea Basic Science Institute in Daejeon, Korea.

SUPPLEMENTAL INFORMATION

Supplemental Information includes Supplemental Experimental Procedures, eight figures, and one table and can be found with this article online at http://dx.doi.org/10.1016/j.celrep.2016.04.064.

AUTHOR CONTRIBUTIONS

S.-Y.L., A.Y.T., and H.W.R. designed the study. S.-Y.L., M.-G.K., and J.-S.P. performed the experiment. S.-Y. L., G.L., and H.-W.R. analyzed data. S.-Y.L., A.Y.T., and H.-W.R. wrote the paper.

ACKNOWLEDGMENTS

This work was supported by NRF (2013R1A1A1057597), the UNIST research fund (1.140101.01), and the Korea Health Technology R&D Project through the Korea Health Industry Development Institute (KHIDI) funded by the Ministry of Health & Welfare of Korea (HI16C0091). Instrumentation was supported by the Samsung Science and Technology Foundation (SSTF-BA1401-11).

Received: November 25, 2015
Revised: March 1, 2016
Accepted: April 17, 2016
Published: May 12, 2016

REFERENCES

Andronicos, N.M., Chen, E.I., Baik, N., Bai, H., Parmer, C.M., Kiosses, W.B., Kamps, M.P., Yates, J.R., 3rd, Parmer, R.J., and Miles, L.A. (2010). Proteomics-based discovery of a novel, structurally unique, and developmentally regulated plasminogen receptor, Plg-RKT, a major regulator of cell surface plasminogen activation. Blood *115*, 1319–1330.

Bendayan, M. (2001). Tech.Sight. Worth its weight in gold. Science *291*, 1363–1365.

Brambillasca, S., Yabal, M., Soffientini, P., Stefanovic, S., Makarow, M., Hegde, R.S., and Borgese, N. (2005). Transmembrane topogenesis of a tail-anchored protein is modulated by membrane lipid composition. EMBO J. *24*, 2533–2542.

Cavdar Koc, E., Burkhart, W., Blackburn, K., Moseley, A., and Spremulli, L.L. (2001). The small subunit of the mammalian mitochondrial ribosome. Identification of the full complement of ribosomal proteins present. J. Biol. Chem. *276*, 19363–19374.

Chen, C.L., Hu, Y., Udeshi, N.D., Lau, T.Y., Wirtz-Peitz, F., He, L., Ting, A.Y., Carr, S.A., and Perrimon, N. (2015). Proteomic mapping in live Drosophila tissues using an engineered ascorbate peroxidase. Proc. Natl. Acad. Sci. USA *112*, 12093–12098.

Colombini, M. (1979). A candidate for the permeability pathway of the outer mitochondrial membrane. Nature *279*, 643–645.

Davis, T.N. (2004). Protein localization in proteomics. Curr. Opin. Chem. Biol. *8*, 49–53.

Fleming, M.D., Campagna, D.R., Haslett, J.N., Trenor, C.C., 3rd, and Andrews, N.C. (2001). A mutation in a mitochondrial transmembrane protein is responsible for the pleiotropic hematological and skeletal phenotype of flexed-tail (f/f) mice. Genes Dev. *15*, 652–657.

Forner, F., Arriaga, E.A., and Mann, M. (2006). Mild protease treatment as a small-scale biochemical method for mitochondria purification and proteomic mapping of cytoplasm-exposed mitochondrial proteins. J. Proteome Res. *5*, 3277–3287.

Friedman, J.R., Webster, B.M., Mastronarde, D.N., Verhey, K.J., and Voeltz, G.K. (2010). ER sliding dynamics and ER-mitochondrial contacts occur on acetylated microtubules. J. Cell Biol. *190*, 363–375.

Gottlieb, Y., Truman, M., Cohen, L.A., Leichtmann-Bardoogo, Y., and Meyron-Holtz, E.G. (2012). Endoplasmic reticulum anchored heme-oxygenase 1 faces the cytosol. Haematologica *97*, 1489–1493.

Guarani, V., McNeill, E.M., Paulo, J.A., Huttlin, E.L., Fröhlich, F., Gygi, S.P., Van Vactor, D., and Harper, J.W. (2015). QIL1 is a novel mitochondrial protein required for MICOS complex stability and cristae morphology. eLife *4*, 4.

Hegde, R.S., and Keenan, R.J. (2011). Tail-anchored membrane protein insertion into the endoplasmic reticulum. Nat. Rev. Mol. Cell Biol. *12*, 787–798.

Heritage, D., and Wonderlin, W.F. (2001). Translocon pores in the endoplasmic reticulum are permeable to a neutral, polar molecule. J. Biol. Chem. *276*, 22655–22662.

Hung, V., Zou, P., Rhee, H.W., Udeshi, N.D., Cracan, V., Svinkina, T., Carr, S.A., Mootha, V.K., and Ting, A.Y. (2014). Proteomic mapping of the human mitochondrial intermembrane space in live cells via ratiometric APEX tagging. Mol. Cell *55*, 332–341.

Jan, Y., Matter, M., Pai, J.T., Chen, Y.L., Pilch, J., Komatsu, M., Ong, E., Fukuda, M., and Ruoslahti, E. (2004). A mitochondrial protein, Bit1, mediates apoptosis regulated by integrins and Groucho/TLE corepressors. Cell *116*, 751–762.

Jing, J., He, L., Sun, A., Quintana, A., Ding, Y., Ma, G., Tan, P., Liang, X., Zheng, X., Chen, L., et al. (2015). Proteomic mapping of ER-PM junctions identifies STIMATE as a regulator of Ca^{2+} influx. Nat. Cell Biol. *17*, 1339–1347.

Kalderon, D., Roberts, B.L., Richardson, W.D., and Smith, A.E. (1984). A short amino acid sequence able to specify nuclear location. Cell *39*, 499–509.

Kim, H., Melén, K., Osterberg, M., and von Heijne, G. (2006). A global topology map of the Saccharomyces cerevisiae membrane proteome. Proc. Natl. Acad. Sci. USA *103*, 11142–11147.

Koc, E.C., Cimen, H., Kumcuoglu, B., Abu, N., Akpinar, G., Haque, M.E., Spremulli, L.L., and Koc, H. (2013). Identification and characterization of CHCHD1, AURKAIP1, and CRIF1 as new members of the mammalian mitochondrial ribosome. Front. Physiol. *4*, 183.

Koch, M., Breithaupt, C., Kiefersauer, R., Freigang, J., Huber, R., and Messerschmidt, A. (2004). Crystal structure of protoporphyrinogen IX oxidase: a key enzyme in haem and chlorophyll biosynthesis. EMBO J. *23*, 1720–1728.

Lam, S.S., Martell, J.D., Kamer, K.J., Deerinck, T.J., Ellisman, M.H., Mootha, V.K., and Ting, A.Y. (2015). Directed evolution of APEX2 for electron microscopy and proximity labeling. Nat. Methods *12*, 51–54.

Lee, H., Min, J., von Heijne, G., and Kim, H. (2012). Glycosylatable GFP as a compartment-specific membrane topology reporter. Biochem. Biophys. Res. Commun. *427*, 780–784.

Lee, K.W., Okot-Kotber, C., LaComb, J.F., and Bogenhagen, D.F. (2013). Mitochondrial ribosomal RNA (rRNA) methyltransferase family members are positioned to modify nascent rRNA in foci near the mitochondrial DNA nucleoid. J. Biol. Chem. *288*, 31386–31399.

Lorenz, H., Hailey, D.W., Wunder, C., and Lippincott-Schwartz, J. (2006). The fluorescence protease protection (FPP) assay to determine protein localization and membrane topology. Nat. Protoc. *1*, 276–279.

Martell, J.D., Deerinck, T.J., Sancak, Y., Poulos, T.L., Mootha, V.K., Sosinsky, G.E., Ellisman, M.H., and Ting, A.Y. (2012). Engineered ascorbate peroxidase as a genetically encoded reporter for electron microscopy. Nat. Biotechnol. *30*, 1143–1148.

Medlock, A.E., Shiferaw, M.T., Marcero, J.R., Vashisht, A.A., Wohlschlegel, J.A., Phillips, J.D., and Dailey, H.A. (2015). Identification of the Mitochondrial Heme Metabolism Complex. PLoS ONE *10*, e0135896.

Mick, D.U., Vukotic, M., Piechura, H., Meyer, H.E., Warscheid, B., Deckers, M., and Rehling, P. (2010). Coa3 and Cox14 are essential for negative feedback regulation of COX1 translation in mitochondria. J. Cell Biol. *191*, 141–154.

Mick, D.U., Rodrigues, R.B., Leib, R.D., Adams, C.M., Chien, A.S., Gygi, S.P., and Nachury, M.V. (2015). Proteomics of primary cilia by proximity labeling. Dev. Cell *35*, 497–512.

Pagliarini, D.J., Calvo, S.E., Chang, B., Sheth, S.A., Vafai, S.B., Ong, S.E., Walford, G.A., Sugiana, C., Boneh, A., Chen, W.K., et al. (2008). A mitochondrial protein compendium elucidates complex I disease biology. Cell *134*, 112–123.

Rees, J.S., Li, X.W., Perrett, S., Lilley, K.S., and Jackson, A.P. (2015). Protein neighbors and proximity proteomics. Mol. Cell. Proteomics *14*, 2848–2856.

Rhee, H.W., Zou, P., Udeshi, N.D., Martell, J.D., Mootha, V.K., Carr, S.A., and Ting, A.Y. (2013). Proteomic mapping of mitochondria in living cells via spatially restricted enzymatic tagging. Science *339*, 1328–1331.

Serrat, R., Mirra, S., Figueiro-Silva, J., Navas-Pérez, E., Quevedo, M., López-Doménech, G., Podlesniy, P., Ulloa, F., Garcia-Fernàndez, J., Trullas, R., and Soriano, E. (2014). The Armc10/SVH gene: genome context, regulation of mitochondrial dynamics and protection against Aβ-induced mitochondrial fragmentation. Cell Death Dis. *5*, e1163.

Shemesh, T., Klemm, R.W., Romano, F.B., Wang, S., Vaughan, J., Zhuang, X., Tukachinsky, H., Kozlov, M.M., and Rapoport, T.A. (2014). A model for the generation and interconversion of ER morphologies. Proc. Natl. Acad. Sci. USA *111*, E5243–E5251.

Shibata, Y., Voeltz, G.K., and Rapoport, T.A. (2006). Rough sheets and smooth tubules. Cell *126*, 435–439.

Shim, S.H., Xia, C., Zhong, G., Babcock, H.P., Vaughan, J.C., Huang, B., Wang, X., Xu, C., Bi, G.Q., and Zhuang, X. (2012). Super-resolution fluorescence imaging of organelles in live cells with photoswitchable membrane probes. Proc. Natl. Acad. Sci. USA *109*, 13978–13983.

Surovtseva, Y.V., Shutt, T.E., Cotney, J., Cimen, H., Chen, S.Y., Koc, E.C., and Shadel, G.S. (2011). Mitochondrial ribosomal protein L12 selectively associates with human mitochondrial RNA polymerase to activate transcription. Proc. Natl. Acad. Sci. USA *108*, 17921–17926.

Takahashi, M., Doré, S., Ferris, C.D., Tomita, T., Sawa, A., Wolosker, H., Borchelt, D.R., Iwatsubo, T., Kim, S.H., Thinakaran, G., et al. (2000). Amyloid precursor proteins inhibit heme oxygenase activity and augment neurotoxicity in Alzheimer's disease. Neuron *28*, 461–473.

Uhlen, M., Oksvold, P., Fagerberg, L., Lundberg, E., Jonasson, K., Forsberg, M., Zwahlen, M., Kampf, C., Wester, K., Hober, S., et al. (2010). Towards a knowledge-based Human Protein Atlas. Nat. Biotechnol. *28*, 1248–1250.

Williams, C.C., Jan, C.H., and Weissman, J.S. (2014). Targeting and plasticity of mitochondrial proteins revealed by proximity-specific ribosome profiling. Science *346*, 748–751.

Yoshida, T., and Sato, M. (1989). Posttranslational and direct integration of heme oxygenase into microsomes. Biochem. Biophys. Res. Commun. *163*, 1086–1092.